

Analysis of insulin amyloid fibrils by Raman spectroscopy

Corasi Ortiz^a, Dongmao Zhang^{a,*}, Alexander E. Ribbe^{a,b}, Yong Xie^a, Dor Ben-Amotz^{a,*}

^a Department of Chemistry, Purdue University, West Lafayette, IN 47907, USA

^b Purdue Laboratory for Chemical Nanotechnology, Purdue University, West Lafayette, IN 47907, USA

Received 1 March 2007; accepted 24 March 2007

Available online 31 March 2007

Abstract

The formation of amyloid fibrils from insulin is investigated using drop-coating-deposition-Raman (DCDR) difference spectroscopy and atomic force microscopy (AFM). Fibrils formed using various co-solvents and heating cycles are found to induce the appearance of Raman difference peaks in the amide I ($\sim 1675\text{ cm}^{-1}$), amide III ($\sim 1220\text{ cm}^{-1}$), and peptide backbone ($\sim 1010\text{ cm}^{-1}$), consistent with an increase in β -sheet content. Comparisons of results obtained from fibrils in either H_2O or D_2O suggest that the NH/ND stretch bands (at $\sim 3300\text{ cm}^{-1}/\sim 2400\text{ cm}^{-1}$) are also enhanced in intensity upon fibril formation. If there is any water trapped in the core of the fibrils its OH/OD Raman intensity is too small to be detected in the presence of the stronger NH/ND bands which appear in the same region. AFM is used to confirm the formation of fibrils of about 5 nm diameter (and various lengths).

© 2007 Elsevier B.V. All rights reserved.

Keywords: Raman; Atomic force microscopy; AFM; DCDR; Protein; Fibril

1. Introduction

Protein activity depends on its native folded structure; as a result, protein misfolding can lead to disease [1]. For instance, degenerative disorders such as Alzheimer's, Parkinson's and type II diabetes are believed to derive from misfolded protein aggregates, known as amyloid fibrils, which build up in organs and tissues [1–5]. Amyloid fibrils share a core cross- β -structure [2,6]. While there are about 20 proteins known to form fibrils *in vivo*, it is believed that many other proteins also have the ability to form these structures [1,2]. Insulin fibrils, for example, have been observed following continuous subcutaneous insulin infusion and repeated insulin injections [2,7]. Insulin fibrillation has been extensively studied in an effort to understand this process [7–10]. Here, we characterize insulin fibrils that are formed under various conditions using Raman spectroscopy, which is exceptionally sensitive to protein secondary structure,

combined with atomic force microscopy (AFM), which is used to directly visualize individual fibrils.

Although Raman spectroscopy can provide structural information about biological systems, its inherently low intensity has historically precluded its applications in biochemical analysis [11,12]. However, with the advent of new methods such as drop coating deposition Raman (DCDR), Raman spectroscopy is no longer limited primarily to liquids or solids with high analyte concentration [13–15]. In particular, the DCDR method has made it possible to rapidly acquire high-quality Raman spectra from dilute protein solutions (down to 1 μM) [13,16], thus significantly expanding the scope of Raman spectroscopic applications in biochemical diagnostics [13,16–20].

Raman spectroscopy has been extensively used for the study of fibrils [21,22]. Early Raman studies of insulin fibrils include important work by Yu and coworkers, who assigned insulin Raman features and demonstrated spectral sensitivity to protein denaturation and fibril formation [21]. Subsequent work has confirmed that insulin fibril formation is marked by the appearance of Raman bands that are characteristic of β -sheet formation, with peaks in the amide I and amide III regions in the vicinity of $\sim 1675\text{ cm}^{-1}$ and $\sim 1220\text{ cm}^{-1}$, respectively (with

* Corresponding authors.

E-mail addresses: Dongmao_zhang@yahoo.com (D. Zhang), dor@purdue.edu (D. Ben-Amotz).

peak position variations of the order of $5\text{--}15\text{ cm}^{-1}$ reported in independent studies). Here, we demonstrate that the DCDR method may be used to obtain high quality Raman spectra of insulin amyloid fibrils. These fibril spectra are compared to those obtained from native insulin, using difference spectroscopy, to clearly identify the Raman spectral signatures associated with fibrillation; two of which are consistent with the above amide I and III signatures, as well as two additional fibrillation signatures, one at $\sim 1010\text{ cm}^{-1}$ (in the peptide backbone region) and the other at $\sim 3300\text{ cm}^{-1}$ (in the amide A region) which have apparently not been previously reported. Moreover, AFM is used to directly verify that fibrils have formed as well as to quantify the dimensions of individual fibrils.

2. Materials and methods

2.1. Sample preparation

Bovine insulin (USP grade) was purchased from Sigma and used without further purification. Insulin fibrils were prepared using the following five different protocols. Insulin (2 mg/mL) was dissolved in the following buffers: 0.1 M HCl, 0.1 M NaCl (pH 1.60); 20% acetic acid, 0.1 M NaCl (pH 2.00); and 20% acetic acid, 1.5 M Guanidine (Gdn.HCl) [7–9]. These solutions were incubated at $50\text{ }^{\circ}\text{C}$ for 20 hours. Insulin fibrils were also prepared by dissolving insulin (50 mg/mL) in 60% ethanol, 0.1 M *tris*-buffer, 2 mM EDTA (pH 7.4) and incubating it at $37\text{ }^{\circ}\text{C}$ for two days [7]. An additional insulin fibril sample was made by heating 1% insulin at pH 2.0 (in HCl) for 2–10 min ($80\text{--}100\text{ }^{\circ}\text{C}$) until a gel was formed. Then, the solution was cooled down, and frozen using a dry ice-acetone bath, followed by thawing of the sample with tap water. These steps were repeated (3–4 times) until a firm gel was formed [7].

Before Raman spectral acquisition, insulin fibrils were centrifuged and washed to remove excess buffer that may interfere with the signal coming from the protein. Fibril suspensions were then usually transferred to a microcentrifuge tube and centrifuged using a HERMLE® Z180M mini-centrifuge (Labnet International) for 30 min at 13,000 rpm. Once the supernatant was removed, the fibrils were resuspended in about 1 mL of pure water. This centrifuge-resuspension procedure was repeated 5 times. Afterwards, the fibril suspensions were deposited onto a SpectRIM® slide (Tienta Sciences Inc.) by pipetting a 3 μL volume of the suspension on to the surface of the slide [13,16]. All the fibril deposits were dried under vacuum as described elsewhere [16]. DCDR spectra were acquired after the deposited samples were visually dry.

Fibril formation was verified using AFM (Digital Instruments/Veeco Multimode Nanoscope IIIa) in tapping mode using a large range scanner and standard silicon tapping mode tips (MicroMash NSC15/BSA1) having a characteristic resonance frequency of about 300 kHz. Image evaluation and representation was done using the open source SPM image manipulation software Gwyddion (gwyddion.net).

2.2. Raman instrumentation and spectral processing

All the DCDR spectra were acquired with a home-built confocal Raman system equipped with a 632.8 nm, 45 mW, He–Ne excitation laser which has been described elsewhere [19]. A $100\times$ objective (NA 0.95, Olympus), which produced a laser spot size of about $1\text{ }\mu\text{m}$, was used to collect the DCDR data and the power at the sample was about 10 mW. To improve the spectral signal-to-noise, all the spectra shown in this work were obtained by adding four 100 s Raman spectra acquired consecutively under the same conditions. Cosmic spikes in the Raman spectra were removed using a variant of the Upper Bound Spectrum (UBS) method implemented using the Matlab programming language [23]. Difference spectra were obtained by adjusting the relative amplitude of the subtracted spectrum so as to minimize the intensity of either the phenylalanine peak at 1000 cm^{-1} or the CH stretching peaks in the 2850 cm^{-1} to 3030 cm^{-1} region.

2.3. Sample preparation for high-frequency Raman

In an effort to verify whether fibrils are water-filled [24], the solvent (H_2O) was exchanged by washing the fibril suspension with deuterated water (D_2O) following the same steps described in Section 2.1. In order to compare hydrogen/deuterium (H/D) exchange with native and fibril insulin, H/D exchanged native insulin was also prepared. A 2 mg insulin sample was dissolved in 1 mL D_2O and, after letting the solution set for 1 hour at room temperature, the insulin solution was freeze-dried. Then 1 mL D_2O was added to the sample, followed by freeze-drying. Finally, 1 mL D_2O was added to the dried sample followed by deposition 3 μL onto a SpectRIM® slide and solvent evaporation, for DCDR measurement.

After acquisition of the DCDR spectra of freshly prepared H/D exchanged native insulin and insulin fibril deposits, the SpectRIM® slide containing these deposits was heated at $110\text{ }^{\circ}\text{C}$ in an oven under vacuum (10^{-3} Torr) for three days to remove all the free D_2O (or H_2O) from the sample, and Raman spectra were acquired after the substrate was cooled under ambient conditions.

3. Results and discussion

3.1. AFM of insulin fibrils

Before DCDR spectra were collected, AFM images were obtained to verify the formation of fibrils. Fig. 1 shows the AFM height image of fibrils prepared by incubating a 2 mg/ml insulin solution in 0.1 M HCl, 0.1 M NaCl (pH 1.60) at $50\text{ }^{\circ}\text{C}$ for 20 h. As evident from the height profile shown in part c of Fig. 1, the diameter of a single rod is about 4.5 nm. The actual diameter is probably 10–20% larger (about 5 nm) due to known compression effects of the AFM tip while scanning in tapping mode. The diameter determined in the lateral direction, perpendicular to the rod, is unreliable due to well known tip convolution effects, especially if the tip radius (typically $>10\text{ nm}$) is much larger than the dimensions of the

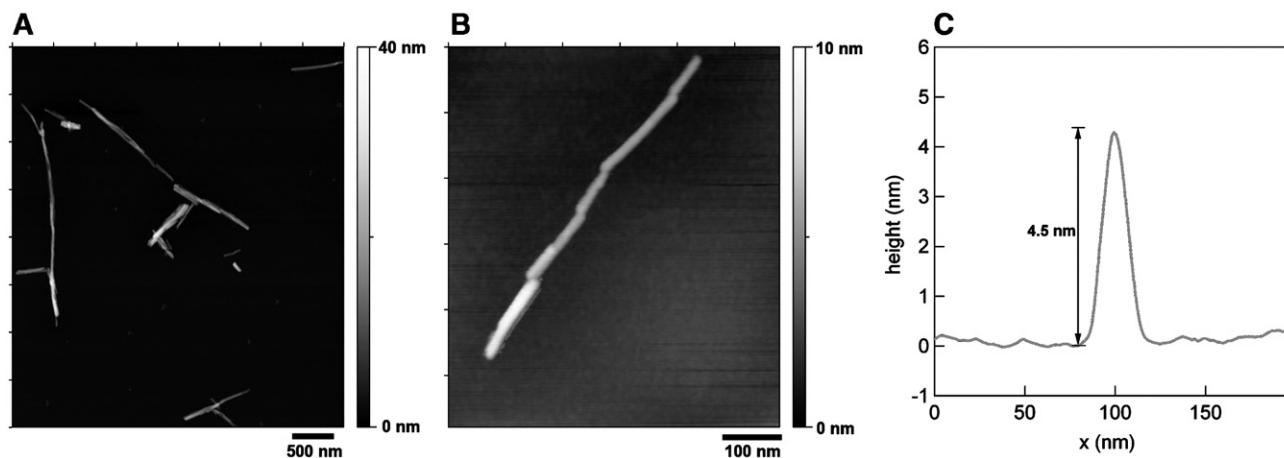


Fig. 1. (A) Oversight and (B) higher resolution tapping mode AFM height images of insulin amyloid fibrils prepared by incubating a 2 mg/mL insulin solution in 20% acetic acid/0.1 M NaCl at 50 °C for 20 h. (C) Average of 30 height profiles with equidistant spacing along a 30 nm long section of one of the fibrils shown in part (B).

investigated structure. It is noteworthy that TEM measurements do not provide any more detailed structural information regarding features such as, for example, the inner diameter of the fibril tube, as demonstrated in studies of other organic based nanotubular systems of similar morphology length and diameter (i.e. outer tube diameter 3–4 nm and inner tube diameter ~ 1 nm) [25]. Note that the measured diameter of the prepared insulin fibrils is consistent with that commonly observed for such filamentous aggregates. Fibrils prepared under other conditions (data not shown) provide similar dimensions (with diameters of 4–6 nm and lengths of 30–140 nm).

3.2. DCDR spectra of insulin fibrils

Fibrils are structures of high β -sheet content. So in the case of insulin, which is mainly α -helical in its native state, we expect to observe significant changes in the DCDR spectra associated with an increase in the β -sheet content of the protein. Fig. 2 shows the DCDR spectra of insulin fibrils formed (A) after incubation in ethanol and (B) by heating a 1% solution (see subsection 2.1). Spectra (a) and (b), in both panels, were obtained from the fibril and native insulin samples, respectively, while spectrum (c) represents the difference between spectra (a) and (b). As expected, various changes are evident throughout

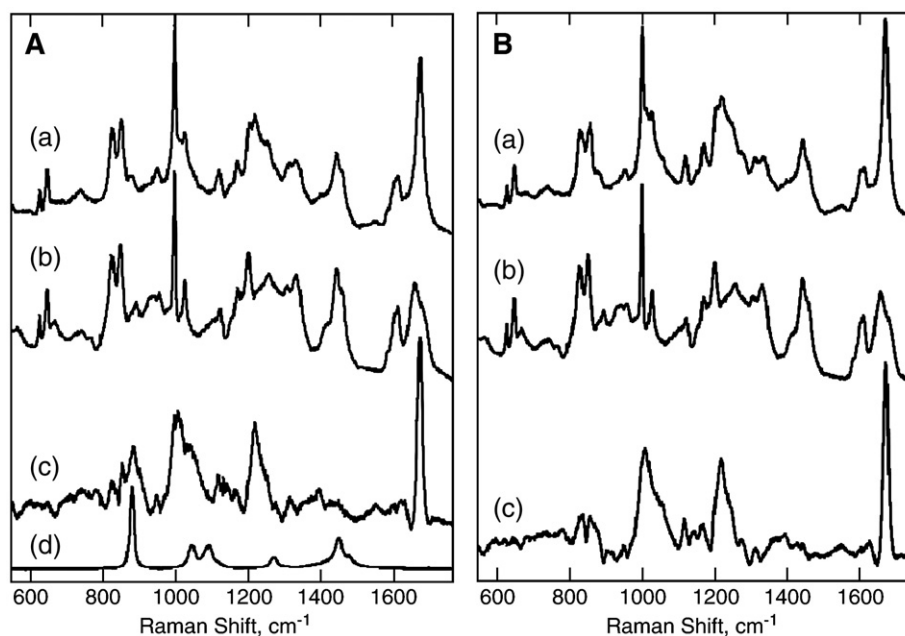


Fig. 2. DCDR spectra of insulin amyloid fibrils (a) and native insulin (b). The fibril spectra in panel A correspond to fibrils prepared in a 60% ethanol solution while the ones in panel B were obtained from fibrils prepared by heat. Spectra (c) in each panel are the corresponding difference spectra whereas (d) in panel A is an ethanol spectrum. The spectra in each panel are plotted using the same vertical scale and offset for clarity.

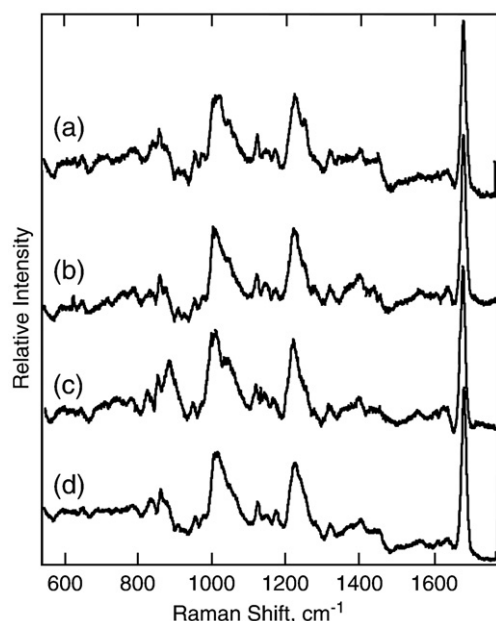


Fig. 3. DCDR difference spectra between insulin amyloid fibrils and native insulin. Fibrils were prepared from insulin solutions in 20% acetic acid/1.5 M guanidine (a), 20% acetic acid (b), 60% ethanol (c), and by heating/freezing/thawing cycles (d). The spectra are plotted using the same vertical scale and offset for clarity.

the spectra. Of particular interest are peaks at $\sim 1675\text{ cm}^{-1}$ and $\sim 1220\text{ cm}^{-1}$ in the amide I and amide III region, respectively, which are consistent with an increase in β -sheet content [21,22]. The difference spectra in Fig. 2 also show an additional change around $\sim 1010\text{ cm}^{-1}$ which we believe reflects changes in the peptide backbone structural upon fibrillation. The additional band in the difference spectra at about 885 cm^{-1} is believed to come from the ethanol used to induce fibril formation, and

whose Raman spectrum (in the pure liquid state) is shown in Fig. 2A(d).

To verify that the predominant spectral changes are indeed associated with fibrillation, we prepared insulin fibrils five different ways. As a further comparison, we also prepared fibrils using other proteins such as lysozyme [16] and ovalbumin (data not shown). Fig. 3 shows the difference between the Raman spectra of different insulin fibrils and native insulin. This figure shows that the Raman fingerprint of fibrillation is independent of the method used for preparation. Similar difference results were obtained upon fibrillation of other proteins [16], strongly suggesting that these spectral changes represent amyloid fibrillation markers.

3.3. High-frequency Raman spectra of fibrils

Fig. 4 shows high frequency Raman spectra of (a) insulin fibrils and (b) native insulin (both obtained after H/D solvent exchange); the spectra in panel A and B were obtained before and after heating under vacuum, respectively (as described in Section 2.3). As evident in panel A, a band at $\sim 2450\text{ cm}^{-1}$ associated with N–D or O–D stretching vibrations can be seen in both of the H/D exchanged fibril and native insulin spectra before heating. The N–D/O–D signal intensity also appears to be higher for native insulin than that for insulin fibril, as evidenced by the negative going peak at $\sim 2500\text{ cm}^{-1}$ in the difference spectrum (c) in panel A. This larger intensity of N–D/O–D in the native insulin may simply indicate that there are more D_2O molecules retained in the insulin monomer deposits than in the fibrils. However, it may also reflect the fact that insulin monomers have greater access to D_2O for H/D exchange than does insulin in the fibril structure.

After heating the deposits under vacuum for 3 days, the signal intensities in the O–D/N–D stretch region indicate that

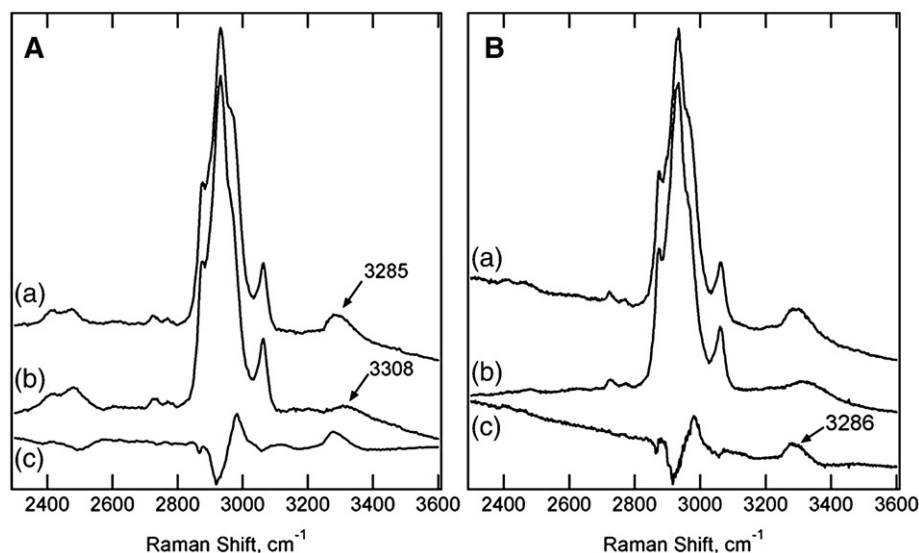


Fig. 4. DCDR spectra of insulin fibrils (a), prepared by incubation in 20% acetic acid at 50°C for 20 h, obtained after $\text{D}_2\text{O}/\text{H}_2\text{O}$ solvent exchange and native insulin (b). The spectra in panel A correspond to protein deposits before heating in an oven at 50°C for 3 days in an oven while the ones in panel B were acquired after heating. The bottom spectra in each panel are the corresponding difference spectra. The spectra in each panel are plotted using the same vertical scale and offset for clarity.

nearly all of the D₂O has evaporated from the native insulin deposit, while there appears to be a small amount of remaining D₂O in the insulin fibril spectrum, as evidenced by the small positive peak in the difference spectrum (c) in panel B. This implies that the peaks at $\sim 2500\text{ cm}^{-1}$ were primarily due to D₂O and that some D₂O is more strongly bound to the insulin fibrils than to the native insulin. On the other hand, approximately the same level of signal intensity of the N–H/O–H stretch region at $\sim 3300\text{ cm}^{-1}$ remains in the fibril spectra. The peaks in this region may represent protein N–H stretches as well as possibly also O–H stretch of water that is trapped in the interior pore of the fibril. The apparently stronger intensity of the band in the $\sim 3300\text{ cm}^{-1}$ region of the insulin fibrils Raman spectrum could reflect the fact that more peptide bonds are involved in hydrogen bonding within the amyloid fibril, thus producing a narrower N–H stretch conformational distribution in the insulin fibrils than that in native insulin, and a sharper amide A band for insulin fibrils. An alternative explanation for all of the above observations may be that, since fibrils are believed to be hollow cylinders or ribbons [26], there are some water molecules trapped in the core of insulin fibrils, as suggested by Perutz et al. [24], and remain inside the fibrils even after extended heating.

In an effort to distinguish the above alternative explanations, we performed additional studies of insulin fibrils formed in a D₂O solution (rather than formed in H₂O followed by washing in D₂O, as above). The resulting fibril DCDR spectra revealed a marked increase in the double band at $\sim 2400\text{ cm}^{-1}$ (and a decrease in the band $\sim 3300\text{ cm}^{-1}$), relative to the corresponding bands in the (a) spectra of Fig. 4. Moreover, the band at $\sim 2400\text{ cm}^{-1}$ no longer decreased significantly upon extended heating. These results confirm that NH/ND bands are enhanced upon fibrillation, and thus that the enhanced Raman intensity of fibrils at $\sim 3300\text{ cm}^{-1}$ which is evident in Fig. 4 is primarily due to NH vibrations (which apparently do not undergo significant H/D exchange upon washing in D₂O). However, these results do not preclude the presence of water in the interior of fibrils, as the amount of trapped water may be sufficiently small that its OH/OD intensity is smaller than the NH/ND bands appearing in the same regions.

4. Conclusion

The results in this work indicate that DCDR spectroscopy is a viable method for the study of protein structural changes, such as fibrillation. We have used difference spectroscopy to clearly reveal four common Raman spectral features associated with insulin fibrillation: (a) a sharp and intense band in the amide I region (at $\sim 1675\text{ cm}^{-1}$), (b) a broader band intense band in the amide III region (at $\sim 1220\text{ cm}^{-1}$), and (c) a broad asymmetric band in the peptide backbone region (at $\sim 1010\text{ cm}^{-1}$), (d) a broad intense band in the amide A region (at $\sim 3300\text{ cm}^{-1}$). The first two features have also been observed in other proteins fibrils, including lysozyme, ovalbumin and β -lactoglobulin-b, and are consistent with an increase in β -sheet content upon fibril formation. These, combined with the latter two bands, which do not appear to have been previously associated with

fibril formation, may prove to be of value as Raman signatures of fibrillation.

We initially wondered whether the band in the amide A region may be due to water trapped inside the fibril core, as suggested by recent theoretical studies [24]. However, our subsequent investigations suggested that the observed amide A Raman band is most likely due to changes in the amide (NH stretch) backbone structure upon fibrillation. More specifically, several experiments were performed by replacing H₂O by D₂O in either the fibril growth or subsequent washing steps, in hopes of seeing evidence of water trapped in the center of the fibril nano-tubes. The results imply that, if water is trapped in fibril interiors, its OH (or OD) Raman intensity is significantly smaller than that of the NH (or ND) bands appearing in the same spectral region.

References

- [1] C.M. Dobson, Trends Biochem. Sci. 24 (1999) 329–332; C.M. Dobson, Philos. Trans. R. Soc. Lond., B Biol. Sci. 356 (2001) 133–145.
- [2] V.N. Uversky, A.L. Fink, Biochim. Biophys. Acta 1698 (2004) 131–153.
- [3] A.C. Dimakopoulos, Curr. Res. Alzheimer's Dis. 2 (2005) 19–28.
- [4] J.D. Sipe, A.S. Cohen, J. Struct. Biol. 130 (2000) 88–98.
- [5] R.L. Hull, G.T. Westermark, P. Westermark, S.E. Kahn, J. Clin. Endocrinol. Metab. 89 (2004) 3629–3643; S.E. Kahn, S. Andrikopoulos, C.B. Verchere, Diabetes 48 (1999) 241–253.
- [6] O.S. Makin, L.C. Serpell, FEBS J. 272 (2005) 5950–5961.
- [7] J. Brange, L. Andersen, E.D. Laursen, G. Meyn, E. Rasmussen, J. Pharm. Sci. 86 (1997) 517–525.
- [8] M.J. Burke, M.A. Rougvie, Biochemistry 11 (1972) 2435–2439.
- [9] L. Nielsen, S. Frokjaer, J. Brange, V.N. Uversky, A.L. Fink, Biochemistry 40 (2001) 8397–8409.
- [10] J.L. Jiménez, E.J. Nettleton, M. Bouchard, C.V. Robinson, C.M. Dobson, H.R. Saibil, PNAS 99 (2002) 9196–9201.
- [11] P.R. Carey, Raman Spectroscopy, J. Biol. Chem. 274 (1999) 26625–26628.
- [12] L.A. Lyon, C.D. Keating, A.P. Fox, B.E. Baker, L. He, S.R. Nicewarmer, S.P. Mulvaney, M.J. Natan, Anal. Chem. 70 (1998) 341R–361R; S.P. Mulvaney, C.D. Keating, Anal. Chem. 72 (2000) 145R–157R.
- [13] D. Zhang, Y. Xie, M.F. Mrozek, C. Ortiz, V.J. Davisson, D. Ben-Amotz, Anal. Chem. 75 (2003) 5703–5709.
- [14] J. Dong, D. Dinakarpandian, P.R. Carey, Appl. Spectrosc. 52 (1998) 1117–1122.
- [15] M.J. Pelletier, R. Altkorn, Anal. Chem. 73 (2001) 1393–1397.
- [16] C. Ortiz, D.M. Zhang, Y. Xie, A.E. Ribbe, D. Ben-Amotz, Anal. Biochem. 353 (2) (2006) 157.
- [17] C. Ortiz, D. Zhang, Y. Xie, V.J. Davisson, D. Ben-Amotz, Anal. Biochem. 332 (2004) 245–252.
- [18] D. Zhang, C. Ortiz, Y. Xie, V.J. Davisson, D. Ben-Amotz, Spectrochim. Acta, Part A 61A (2005) 471–475; Y. Xie, D. Zhang, G.K. Jarori, V.J. Davisson, D. Ben-Amotz, Anal. Biochem. 332 (2004) 116–121.
- [19] Y. Xie, Y. Jiang, D. Ben-Amotz, Anal. Biochem. 343 (2005) 223–230.
- [20] M.F. Mrozek, D. Zhang, D. Ben-Amotz, Carbohydr. Res. 339 (2004) 141–145.
- [21] N.-Y. Yu, C. Liu, D.C. O'Shea, J. Mol. Biol. 70 (1972) 117–132; N.-Y. Yu, B.H. Jo, R.C.C. Chang, J.D. Huber, Arch. Biochem. Biophys. 160 (1974) 614–622.
- [22] M.M. Apetri, N.C. Maiti, M.C. Zagorski, P.R. Carey, V.E. Anderson, J. Mol. Biol. 355 (2006) 63–71; J. Dong, Z. Wan, M. Popov, P.R. Carey, M.A. Weiss, J. Mol. Biol. 330 (2003) 431–442; H. Hiramatsu, Y. Goto, H. Naiki, T. Kitagawa, JACS 127 (2005) 7988–7989;

- W.S. Gosal, A.H. Clark, S.B. Ross-Murphy, *Biomacromolecules* 5 (2004) 2408–2419.
- [23] D. Zhang, J.D. Hanna, D. Ben-Amotz, *Appl. Spectrosc.* 57 (2003) 1303–1305;
D. Zhang, D. Ben-Amotz, *Appl. Spectrosc.* 56 (2002) 91–98;
D. Zhang, K.N. Jallad, D. Ben-Amotz, *Appl. Spectrosc.* 55 (2001) 1523–1531.
- [24] M.F. Perutz, J.T. Finch, J. Berriman, A. Lesk, *PNAS* 99 (2002) 5591–5595.
- [25] H. Fenniri, B.-L. Deng, A.E. Ribbe, K. Hallenga, J. Jacob, P. Thiyagarajan, *PNAS* 99 (2002) 6487–6492;
H. Fenniri, B.-L. Deng, A.E. Ribbe, *JACS* 124 (2002) 11064–11072.
- [26] L.C. Serpell, M. Sunde, P.E. Fraser, P.K. Luther, E.P. Morris, O. Sangren, E. Lundgren, C.C.F. Blake, *J. Mol. Biol.* 254 (1995) 113–118;
S.H. Waterhouse, J.A. Gerrard, *Aust. J. Chem.* 57 (2004) 519–523;
S. Gilead, E. Gazit, *Supramol. Chem.* 17 (2005) 87–92.